

1 Improving abundance index for Sol8c9a stock
2 assessment model calibration.

3 Working document to the Working Group for the Bay of Biscay and the
4 Iberian Waters Ecoregion WGBIE – 6-13 May 2020.

5 Maria Grazia Pennino¹, Francisco Izquierdo¹, Marta Cousido¹, Santiago
6 Cerviño¹, Iosu Paradinas², Francisco Velasco³, Jaime Otero¹, Rafael
7 Bañón⁴, and Alex Alonso-Fernández⁴

8 ¹Instituto Español de Oceanografía (IEO), Centro Oceanográfico de Vigo,
9 Subida a Radio Faro 50-52, 36390, Vigo, Pontevedra, Spain.

10 ²Ipar Perspective Asociación, Karabiondo Kalea. 48600 Sopela, Spain

11 ³Instituto Español de Oceanografía, Promontorio San Martín s/n, 39004,
12 Santander, Spain.

13 ⁴Instituto de Investigaciones Marinas, Rúa de Eduardo Cabello, 6, 36208
14 Vigo, Pontevedra, Spain.

15 May 8, 2020

16 **Contents**

17	Abstract	2
18	Introduction	2
19	Material and Methods	4
20	Abundance data	4
21	Fishery-independent data	4
22	Fishery-dependent data	4
23	Modelling abundance data	5
24	Fishery-independent data	5
25	Fishery-dependent data	6
26	Model selection	7
27	SPiCT, stochastic surplus production model in continuous time	7

28	Results	8
29	Fishery-independent data	8
30	Fishery-dependent data	8
31	Abundance indices	9
32	SPiCT	9
33	Conclusions	9
34	Acknowledgments	10
35	Tables	12
36	Figures	14
37	Appendix	26

38 Abstract

39 Time series of abundance indices are the main source of information to calibrate stock as-
40 sessment models. Precise abundance indices are essential for successful conservation and
41 management of fish stocks. Commonly, scientific standardized surveys are used for this aim
42 and to ensure that estimates are unbiased. However, the accuracy of these estimated indices
43 may be low under certain circumstances. In particular the common sole (*Solea solea*) is
44 a species with a biological bathymetric range between 0 and 200 meters in the Iberian At-
45 lantic waters. The annual scientific survey that collects data for demersal species in this area
46 only cover partially this bathymetric range and the resultant abundance indexes are con-
47 sequently underestimated. In addition, habitat variables, (i.e., bathymetry), can influence
48 these estimates as well as the species spatio-temporal variability. Alternatively, standard-
49 ized CPUEs (catch per unit effort) derived fishery-dependent data can be used as a proxy of
50 the species abundance. In this study two different spatio-temporal abundances indices were
51 computed and the impacts on the common sole evaluation using as stock assessment model
52 the SPiCT (stochastic surplus production model in continuous time) were analyzed. Both
53 abundance indices were produced using Bayesian hierarchical spatio-temporal models, con-
54 sidering bathymetry as an environmental variable and testing three different spatio-temporal
55 structures (i.e. opportunistic, progressive and persistent) to categorize the spatio-temporal
56 behaviour of the sole. We argue that using explicitly spatio-temporal abundance indexes can
57 improve the assessment of stocks and in particular for the ones that are in a data-limited
58 situation.

59 Introduction

60 Fishery independent surveys provide important information for species stock assessment
61 and consequently for fisheries management (Cao et al., 2017). Abundance indices are one of
62 the primary information derived from scientific surveys, and are essential to calibrate species

63 stock assessment models. Therefore the accuracy of the abundance indices is essential for the
64 stocks evaluation and the subsequent management decisions (e.g., total allowable catches).

65 Commonly scientific surveys are designed with randomized sampling locations and to
66 ensure that estimates, as abundance indices, are unbiased. However, under certain circum-
67 stances, surveys may produce imprecise estimates of abundance, particularly for species with
68 preferential habitats that are in strata only partially included in the survey sampling design.
69 Therefore, in these cases, the spatial species variation is not adequately captured.

70 The common sole (*Solea solea*) is a species with a biological bathymetric range between
71 0 and 200 meters in the Iberian Atlantic waters. The annual scientific survey that collects
72 data for demersal species in this area only cover partially the sole bathymetric range and
73 the resultant abundance index is probably underestimated.

74 Recently, spatio-temporal models have been implemented to produce more precise abun-
75 dance indices than the ones provided by conventional surveys (Cao et al., 2017; Thorson,
76 2015). Indeed, spatio-temporal models can overcome this problem as they link information
77 on the abundance or presence/absence of a species to the space to predict where (and how
78 much of) a species is likely to be present in unsampled locations elsewhere in a area or
79 period of time (Pennino et al., 2019). Additionally, spatio-temporal models can include as
80 covariates environmental variables, (e.g. bathymetry, temperature, salinity, etc.) and poten-
81 tially generate more precise estimates of abundance, especially when the underlying species
82 distribution is dependent on habitat features.

83 Different studies have applied spatio-temporal models to improve abundance indices (Cao
84 et al., 2017; Shelton et al., 2014; Thorson, 2015). For example, Thorson (2015) implemented
85 spatio-temporal models to compare the abundance indices of 28 groundfish species off the
86 U.S. West Coast with conventional surveys indices. Overall, abundance indices showed
87 similar trends but the uncertainty associated with the spatio-temporal indices was widely
88 lower than the one of conventional indices.

89 Alternatively, fishery-dependent data collected from fishery observers on-board commer-
90 cial vessels or logbooks can be used to construct standardized indices of relative abundance
91 for stock assessment models (Alonso-Fernández et al., 2019). Several standardization tech-
92 niques have been used for fishery-dependent data of many species (Campbell, 2015; Maunder
93 and Punt, 2004), including also environmental variables and spatio-temporal effects (Alonso-
94 Fernández et al., 2019; Teo and Block, 2010). Overall these methods have been proved to be
95 a useful tool to address ecological and assessment issues, especially in data limited situations
96 (Alonso-Fernández et al., 2019).

97 However, few studies showed the impact of using a spatio-temporal index in stock as-
98 sessment models and the derived performance. Recently, Cao et al. (2017) did this exercise
99 for the northern shrimp (*Pandalus borealis*) in the Gulf of Maine. Results of this study
100 showed that using the spatio-temporal index in the assessment model alters the estimates of
101 recruitment and spawning stock biomass, as well as the determination of the stock status.
102 Also, the inclusion of the spatio-temporal index in the assessment improved the predictive
103 performance of the model reducing the retrospective bias.

104 Given that the abundance index provides primary information for stock assessment, such
105 studies are essential to better understand the practical improvement of spatio-temporal index
106 standardization.

107 Within this context, in this study two different spatio-temporal abundance indices were

108 produced using (1) a fishery-independent data-set from 2001-2019 collected through scientific
109 trawl surveys; and (2) a fishery-dependent data-set collected by observers on-board artisanal
110 fisheries vessels from 2000-2018. Both data-sets were analyzed using a Bayesian hierarchical
111 spatio-temporal models, considering bathymetry as an environmental variable.

112 Produced indices were included in the common sole SPiCT (stochastic surplus production
113 model in continuous time) stock assessment model and performance were explored.

114 We argue that using explicitly spatio-temporal abundance indices can improve the as-
115 sessment of stocks and in particular for the ones that are in a data-limited situation.

116 **Material and Methods**

117 **Abundance data**

118 **Fishery-independent data**

119 Fishery-independent data were collected during the scientific survey series “SP-NSGFS Q4”
120 by the “Instituto Español de Oceanografía” (IEO) carried out in autumn (September to
121 October) from 2001 to 2019. The “SP-NSGFS Q4” survey makes use of a stratified sampling
122 design based on depth with three bathymetric strata: 70–120 m, 121–200 m and 201–500 m.
123 Sampling stations consisted of 30 min trawling hauls located randomly within each stratum at
124 the beginning of the design (Figure 1). Approximately 115 hauls divided between the three
125 bathymetric strata were performed every year in this zone, using the baka 44/60 gear and
126 following the protocol of the International Bottom Trawl Survey Working Group (IBTSWG)
127 of ICES (ICES, 2017). Due to the high number of zeros only the first two bathymetric strata
128 (i.e., 70–120 m, 121–200 m) were considered in this study, that correspond with the common
129 sole bathymetric biological range.

130 Two different variables were analyzed in order to characterize the spatio-temporal behav-
131 ior of common sole individuals. First, we considered a presence/absence variable to measure
132 the occurrence probability of the species. Secondly, we used the weight by haul (kg) as an
133 indicator of the conditional-to-presence abundance of the species.

134 **Fishery-dependent data**

135 Fishery-dependent data were collected by the Galician government Technical Unit of Ar-
136 tisanal Fisheries (Unidade Técnica de Pesca de Baixura, UTPB, in Galician). Usually an
137 on-board observer is assigned to fishing vessels randomly selected from this sector and covers
138 the full set of multiple gears used in Galician waters and all along the geographical range
139 (Figure 2). In a single trip each vessel usually performs several hauls. At each haul, ob-
140 servers record all basic operational data (i.e., date, geographical position, gear, etc.) and the
141 number and weight of all retained and discarded taxa. The analysed database in this study
142 counts 4350 hauls for which common sole was caught from January 2000 until December
143 2018.

144 Before fitting any model, we selected the data for the trammel net which is the most
145 representative gear for the common sole in order to reduce sources of variation. This selection
146 was based on three criteria: i) proportion of hauls with zero catch, ii) total number of

147 individuals sampled and iii) the spatio-temporal coverage. The first and second criterion
148 were used as proxies of gear catchability and thus constant catchability was assumed along
149 the time series (Alonso-Fernández et al., 2019).

150 **Modelling abundance data**

151 **Fishery-independent data**

152 The annual scientific survey that collects data for demersal species in the studied area
153 only cover partially the common sole bathymetric range and the resultant abundance in-
154 dex presents a large proportions of zeros observed, i.e., zero inflated data. This data is
155 commonly analysed using two-part models, also known as delta models. Generally, both oc-
156 currence and abundance are modelled through independent models. However, the abundance
157 and occurrence processes are often related, thus violating the independence assumption of
158 common delta models. In this study we applied hurdle Bayesian spatio-temporal models
159 that fitted simultaneously the common sole occurrence and conditional-to-presence abun-
160 dance processes sharing bathymetry effects. These effects were incorporated as described in
161 Paradinas et al. (2017) in order to incorporate information on both the occurrence and the
162 abundance to better fit informed environmental effects.

163 Bathymetry values were retrieved from the European Marine Observation and Data Net-
164 work (EMODnet, <http://www.emodnet.eu/>) with a spatial resolution of 0.02 x 0.02 decimal
165 degrees (20 m).

166 Models were fitted using the integrated nested Laplace approximation approach (Rue
167 et al., 2009) in the R (R Core Team, 2017) software. For the spatial component the spatial
168 partial differential equations (SPDE) module (Lindgren et al., 2011) of INLA was imple-
169 mented. With the SPDE, the spatial field (W_s) was modelled as a multivariate normal
170 distribution with zero mean and a Matérn covariance function that depend on its range (r_w)
171 and variance (σ_w).

172 Additionally, in order to categorize the spatio-temporal behaviour of the common sole,
173 three different spatio-temporal structures were compared (Paradinas et al., 2017) (see Ta-
174 ble 1). In particular, opportunistic structures indicate that species change their spatial
175 pattern every year without following any specific pattern. Persistent structures imply that
176 species have a spatial distribution that does not change every year, while the progressive
177 ones indicate that the spatial pattern changes in a correlated way from one year to another.
178 The progressive structure contains an autoregressive ρ_t parameter that controls the degree
179 of autocorrelation between consecutive years. This ρ_t parameter is bounded to $[0, 1]$, where
180 parameter values close to 0 represent more opportunistic behaviors and parameter values
181 close to 1 represent more persistent distributions along time. We also included an extra tem-
182 poral effect f_t using a second order random walk (RW2) effect to infer any mean intensity
183 changes over time.

184 For each spatio-temporal model we considered Y_{st} and Z_{st} that denote, respectively, the
185 spatio-temporally distributed occurrence and the conditional-to-presence abundance, where
186 $s = 1, \dots, n_t$ is the spatial location and $t = 1, \dots, T$ the temporal index, being $i = 1, \dots, I$ the
187 bathymetry in location s . Occurrence Y_{st} , was modeled using a Bernoulli distribution with
188 a logit link and conditional-to-presence abundance, Z_{st} , with a gamma distribution with a

189 log link, to capture the overdispersion of the data. Then:

$$\begin{aligned}
 Y_{st} &\sim \text{Ber}(\pi_{st}) \\
 Z_{st} &\sim \text{Gamma}(\mu_{st}, \phi_{st}) \\
 \text{logit}(\pi_{st}) &= \alpha^{(Y)} + f_i(d_{ist}) + U_{st}^{(Y)} \\
 \log(\mu_{st}) &= \alpha^{(Z)} + \theta_i f_i(d_{ist}) + U_{st}^{(Z)}
 \end{aligned}
 \tag{1}$$

190 where π_{st} represents the probability of occurrence at location s at time t and μ_{st} and ϕ_{st} are
 191 the mean and dispersion of the conditional-to-presence abundance. The linear predictors,
 192 which contain the effects that link the parameters π_{st} and μ_{st} include: $\alpha^{(Y)}$ and $\alpha^{(Z)}$, that
 193 represent the intercepts of each respective variable; $f_i(d_{ist})$ is the bathymetric effect modelled
 194 as a RW2 smooth function that allow us to fit any possible non-linear relationship of the
 195 bathymetry (Fahrmeir and Lang, 2001) and it is scaled by θ_i to allow for differences in scale
 196 across the different linear predictors in shared effects; the final terms $U_{st}^{(Y)}$ and $U_{st}^{(Z)}$ refer
 197 to the spatio-temporal structure of the occurrence and conditional-to-presence abundance
 198 respectively and may follow any of the three spatio-temporal structures described above.

199 Fishery-dependent data

200 Similarly to the precedent abundance data, the fishery-depended data-set was analyzed using
 201 Bayesian spatio-temporal models with a gamma distribution and log link. All the spatio-
 202 temporal structures were tested and the bathymetry was included as possible predictor and
 203 fitted using a RW2 model. In order to capture the intra-annual variability of this abundance
 204 index, the month of the fishery haul was also included in the model as fixed effect.

205 Fishing effort was included as the duration of gear deployment (i.e. soak time). As it
 206 is known that gear saturation can exert a significant nonlinear effect on catchability this
 207 variable was included as continuous explanatory variable (in minutes, log transformed).
 208 The remaining potential source of abundance variability could be due to differences among
 209 vessels caused by a skipper effect or unobserved gear characteristics. To remove bias caused
 210 by vessel-specific differences in fishing operation, we included a vessel random effect.

211 The Bayesian approach requires the assignation of prior distributions to every parameter
 212 of the model. For both fishery-independent and depended data-sets, vague prior distributions
 213 with a zero-mean and a standard deviation of 100 were implemented for all the fixed effects,
 214 the variance of the abundance process, and the scaling parameter (θ) of the shared effects.
 215 For the geostatistical terms and the ρ parameters of the of the second order random walks
 216 penalised complexity priors (PC priors, weak informative priors) (Fuglstad et al., 2018)
 217 were assigned. Specifically, we used PC priors that satisfied the following criteria: 1) the
 218 probability that the spatial effect range was smaller than 150 km was 0.15, to avoid very
 219 small spatial autocorrelation ranges, 2) the probability that the spatial effect variance was
 220 greater than 1 was 0.20, to avoid masking the bathymetric effect through the spatial effect,
 221 and 3) the probability that ρ was greater than 0.5 in the occurrence model and greater than
 222 the observed abundance standard deviation in the abundance model were 0.01. A sensitivity
 223 analysis of the choice of priors was performed by verifying that the posterior distributions
 224 concentrated well within the support of the priors.

225 **Model selection**

226 In both cases, model selection was performed testing all possible combinations among the
227 possible spatio-temporal structures and variables and using the Watanabe Akaike Informa-
228 tion Criterion (WAIC) (Watanabe, 2010) as criteria of the goodness of fit and the Log-
229 Conditional Predictive Ordinates (LCPO) (Roos et al., 2011) as predictive quality measures.
230 For both measures, the smaller the score the better the model.

231 **SPiCT, stochastic surplus production model in continuous time**

232 The SPiCT explicitly models both abundance and fishing dynamics as stochastic processes
233 in a state-space framework. It is formulated as a continuous time model to allow a repre-
234 sentation of seasonal fishing patterns and incorporation of sub-annual catch and index data
235 Pedersen and Berg (2017).

236 The most important input for fitting SPiCT is catch data (by weight). Pedersen and Berg
237 (2017) define the catch as the product of instantaneous fishing mortality and stock biomass.
238 Fishing mortality is not decomposed into the product of effort and catchability. Therefore,
239 it is not necessary to standardise the catch data based on changes in fishing efficiency: all
240 such changes will be encompassed in the instantaneous fishing mortality.

241 Here we used as catch data the common sole official landings provided by Portugal and
242 Spain in ICES divisions 8.c and 9.a (Figure 3) (2000-2019). For this time-series the ob-
243 servation noise was not constant in time. Indeed, there is some evidence that the common
244 sole catch could be misclassified in the past, which means that common sole official landings
245 might not then have corresponded only to this species but a mix of *Solea solea*, *Solea sene-*
246 *galensis* and *Pegusa lascaris*. Using port sampling length data it was possible to separate the
247 Solea spp. landings and apply the proportions to provide a raised landings for the common
248 sole. However, as in the SPiCT it is possible to add knowledge that certain data points are
249 more uncertain than others, the first 10 years of the catch were considered uncertain relative
250 to the remaining time series and therefore are scaled by a factor 5. In particular using the
251 *stdevfacC* vector that contains the factor that is multiplied onto the standard deviation of
252 the data points of the corresponding observation vector.

253 Catch data must be supplemented in the SPiCT model by at least one independent abun-
254 dance index. An important advantage of SPiCT over other surplus production models is that
255 it allows the use of multiple abundance indices with different time-series in addition to the
256 catch time series. Here we performed three different runs using: 1) only the spatio-temporal
257 abundance index produced with fishery-independent data; 2) only the spatio-temporal abun-
258 dance index produced with fishery-dependent data; 3) both produced spatio-temporal abun-
259 dance indices.

260 The continuous-time SPiCT formulation, time-stepping is achieved through an Euler
261 scheme with a default time increment dt_{Euler} equal to 1/16 (where time is measured in
262 years). As common sole catch data were collected annually, the discrete-time realisation of
263 SPiCT, obtained by setting the time-step dt_{Euler} equal to one, was considered sufficient.

264 For the ratios between observation and process error for abundance and fishing dynamics,
265 α and β , we specified priors vaguely informative priors as recommended by Pedersen and
266 Berg (2017). Optimisation of the model fit is achieved using log-likelihood functions so that

267 many variables and parameters are log-transformed as standard. Therefore, $\log \alpha$ and $\log \beta$
268 were assumed to have normal distributions with mean values of $\log 1$ and standard deviations
269 equal to 2.

270 Production curve shape parameter n was allowed to vary during optimisation and we
271 prescribed a vaguely informative prior normal distribution for $\log n$ with a mean of $\log 2$
272 (corresponding to the logistic curve) and standard deviation 2. These prior specifications
273 are considered a fair reflection of our prior knowledge of the system. The SPiCT model fit
274 is relatively insensitive to increases in the standard deviation of the lognormal distributions;
275 a standard deviation of 10 did not cause any visible changes in the biomass and fishing
276 mortality trends. No other prior information was available regarding the fishing process or
277 biomass production.

278 Model and post-processing R code R Core Team (2017) supplied by Pedersen and Berg
279 (2017) was used to fit the model and analyze the results.

280 Results

281 Fishery-independent data

282 According to model selection scores (see Table 2), the occurrence and abundance distri-
283 butions of the common sole were progressive. Persistent model scores were quite close to
284 the progressive structure, suggesting that distributions were relatively persistent between
285 2001 and 2019. These results were supported by the strong temporal correlation parameters
286 in the progressive spatio-temporal model (0.98 and 0.96 for the occurrence and abundance
287 processes, respectively).

288 The predicted bathymetric distribution of occurrence and abundance revealed a clear
289 decrease with depth from 60 m (Figure 4). Bathymetry explained 41% of spatio-temporal
290 variation of the abundance process, which suggests that this habitat variable has an impor-
291 tant impact on spatial variation in common sole density.

292 The overall abundance of the common sole shows a slightly increasing trend (Figure 5).
293 Note that the marginal temporal effect of Figure 5 is in the log scale.

294 Occurrence and abundance maps (Figures 6 and 7 respectively) highlight two main
295 preferential habitats for the common sole, located over the continental shelf in front of La
296 Coruña and Bilbao cities. It worth to be mentioned that the predictions did not include the
297 extra temporal effect f_t RW2.

298 Fishery-dependent data

299 Model selection scores (see Table 3) show that the abundance distribution of the common
300 sole was progressive. The ρ parameter was 0.45, suggesting more opportunistic distributions
301 (i.e., uncorrelated distributions between years).

302 The predicted bathymetric distribution revealed an increasing abundance trend until 100
303 m and then a decreasing pattern (Figure 8). Bathymetry explained 31% of spatio-temporal
304 variation of the abundance process.

305 The overall abundance of the common sole shows a slightly decreasing trend (Figure 9).
306 Note that the marginal temporal effect of Figure 9 is in the log scale.

307 Abundance maps (Figure 10) highlight not persistent hot-spots but overall two main
308 preferential habitats for the common sole can be identified. They are located one in front of
309 La Coruña city and another in the northern part of the area in front of the Ria do Viveiro.
310 Also in this case, it worth to be mentioned that the predictions did not include the extra
311 temporal effect f_t RW2.

312 Abundance indices

313 When the produced spatio-temporal abundance indices are compared with the observed
314 data, in both cases it is possible to see that temporal tendencies are maintained but more
315 smoothed indices are obtained (Figures 11 and 12). However both indices showed significant
316 correlation with observer data, 0.65 with fishery-independent data and 0.70 for fishery-
317 dependent.

318 SPiCT

319 For the three runs the assessment converged and all the variance parameters of the model
320 were finite as recommended by Pedersen and Berg (2017). However in the three cases
321 some of the model assumptions based on one-step-ahead residuals (i.e. auto-correlation and
322 normality) were violated (Figures 13, 14 and 15). It worth to be mentioned that slight
323 violations of this assumptions do not necessarily invalidate model results (Mildenberger et al.,
324 2020).

325 Table 4 shows the model parameter estimates with 95% confidence intervals for all the
326 models. Results are very different among models and the 95% confidence intervals are very
327 wide.

328 Conclusions

329 Overall the inclusion of the spatio-temporal indices improved the results of the SPiCT model.
330 Indeed before the standardization of the indices (i.e. using observed data) the SPiCT model
331 did not converge at all. However results are very preliminary and they need to be improved.
332 Future steps will be:

333 1) improving the standardization of the fishery-independent and dependent data. For the
334 fishery-dependet data standardization could be improved adding seasonal trends and more
335 effort information.

336 2) include in the predictions and consequent abundance indices the extra temporal effect
337 f_t RW2.

338 3) Pedersen and Berg (2017) outline that the SPiCT formulation describes the dynamics
339 of the exploited part of the fish stock. Therefore, abundance index need to be modified to
340 include only the size-classes exploited by fishery.

341 4) sensitive analysis for the production curve skewness parameter n need to be performed.

Acknowledgments

The authors express their gratitude to all the people that work in the SP-NSGFS Q4 surveys. SP-NSGFS Q4 surveys were co-funded by the EU within the Spanish national program for the collection, management and use of data in the fisheries sector and support for scientific advice regarding the Common Fisheries Policy. This study is indebted with all the on-board observers that carried out the sampling, and with the UTPB that runs the monitoring program of the artisanal fishery sector in Galician waters. This study is a contribution to the project IMPRESS (RTI2018-099868-B-I00) project, ERDF, Ministry of Science, Innovation and Universities - State Research Agency.

References

References

- Alonso-Fernández, A., Otero, J., Bañón, R., Campelos, J. M., Quintero, F., Ribó, J., Filgueira, F., Juncal, L., Lamas, F., Gancedo, A., et al. (2019). Inferring abundance trends of key species from a highly developed small-scale fishery off ne atlantic. *Fisheries Research*, 209:101–116.
- Campbell, R. A. (2015). Constructing stock abundance indices from catch and effort data: some nuts and bolts. *Fisheries Research*, 161:109–130.
- Cao, J., Thorson, J. T., Richards, R. A., and Chen, Y. (2017). Spatiotemporal index standardization improves the stock assessment of northern shrimp in the gulf of maine. *Canadian Journal of Fisheries and Aquatic Sciences*, 74(11):1781–1793.
- Fahrmeir, L. and Lang, S. (2001). Bayesian inference for generalized additive mixed models based on markov random field priors. *Journal of the Royal Statistical Society: Series C (Applied Statistics)*, 50(2):201–220.
- Fuglstad, G.-A., Simpson, D., Lindgren, F., and Rue, H. (2018). Constructing priors that penalize the complexity of gaussian random fields. *Journal of the American Statistical Association*, pages 1–8.
- ICES (2017). Manual of the ibts north eastern atlantic surveys. *Series of ICES Survey Protocols SISP*, 15:92 pp.
- Lindgren, F., Rue, H., and Lindström, J. (2011). An explicit link between gaussian fields and gaussian markov random fields: the stochastic partial differential equation approach. *Journal of the Royal Statistical Society: Series B (Statistical Methodology)*, 73(4):423–498.
- Maunder, M. N. and Punt, A. E. (2004). Standardizing catch and effort data: a review of recent approaches. *Fisheries research*, 70(2-3):141–159.

- 375 Mildenberger, T. K., Berg, C. W., Pedersen, M. W., Kokkalis, A., and Nielsen, J. R. (2020).
376 Time-variant productivity in biomass dynamic models on seasonal and long-term scales.
377 *ICES Journal of Marine Science*, 77(1):174–187.
- 378 Paradinas, I., Conesa, D., López-Quílez, A., and Bellido, J. M. (2017). Spatio-temporal
379 model structures with shared components for semi-continuous species distribution mod-
380 elling. *Spatial Statistics*, 22:434–450.
- 381 Pedersen, M. W. and Berg, C. W. (2017). A stochastic surplus production model in contin-
382 uous time. *Fish and Fisheries*, 18(2):226–243.
- 383 Pennino, M. G., Paradinas, I., Illian, J. B., Muñoz, F., Bellido, J. M., López-Quílez, A., and
384 Conesa, D. (2019). Accounting for preferential sampling in species distribution models.
385 *Ecology and evolution*, 9(1):653–663.
- 386 R Core Team (2017). *R: A Language and Environment for Statistical Computing*. R Foun-
387 dation for Statistical Computing, Vienna, Austria.
- 388 Roos, M., Held, L., et al. (2011). Sensitivity analysis in bayesian generalized linear mixed
389 models for binary data. *Bayesian Analysis*, 6(2):259–278.
- 390 Rue, H., Martino, S., and Chopin, N. (2009). Implementing approximate bayesian inference
391 using integrated nested laplace approximation: A manual for the inla program. *Department*
392 *of Mathematical Sciences, NTNU, Norway*.
- 393 Shelton, A. O., Thorson, J. T., Ward, E. J., and Feist, B. E. (2014). Spatial semiparametric
394 models improve estimates of species abundance and distribution. *Canadian Journal of*
395 *Fisheries and Aquatic Sciences*, 71(11):1655–1666.
- 396 Teo, S. L. and Block, B. A. (2010). Comparative influence of ocean conditions on yellowfin
397 and atlantic bluefin tuna catch from longlines in the gulf of mexico. *PLoS One*, 5(5).
- 398 Thorson, J. T. (2015). Spatio-temporal variation in fish condition is not consistently ex-
399 plained by density, temperature, or season for california current groundfishes. *Marine*
400 *Ecology Progress Series*, 526:101–112.
- 401 Watanabe, S. (2010). Asymptotic equivalence of bayes cross validation and widely applicable
402 information criterion in singular learning theory. *Journal of Machine Learning Research*,
403 11(Dec):3571–3594.

Tables

Model	Notation	Description
Opportunistic	$U_{st} = \mathbf{W}_t$	Different and uncorrelated realizations of the spatial field every year.
Persistent	$U_{st} = \mathbf{W} + f(t)$	A common realization of the spatial field for all years and an additive temporal trend $f(t)$
Progressive	$U_{st} = \mathbf{W}_t + \rho U_{st-1}$	Spatial realizations change over time through a first order autoregressive model. ρ controls the level of correlation between subsequent time events.

Table 1: Summary of fitted spatio-temporal models U_{st} . \mathbf{W} represents a geostatistical spatial field, $f(t)$ is a temporal trend function and ρ is an autoregressive correlation parameter bounded to $[0,1]$.

Model	WAIC	LCPO	Time (sec.)
Persistent structure	1732.17	0.52	128.23
Opportunistic structure	1770.42	0.54	121.57
Progressive structure	1728.22	0.61	7882.21

Table 2: Spatio-temporal structures comparison for the conditional-to-presence abundance distribution of common sole model fishery-independent data based on WAIC and LCPO scores. Time scores refer only to the estimation process of the model. The best model is highlighted in bold.

Model	WAIC	LCPO	Time (sec.)
Persistent structure	57602.89	6.62	102.05
Opportunistic structure	57685.80	6.63	107.175
Progressive structure	57290.89	6.50	834.471

Table 3: Spatio-temporal structures comparison for abundance distribution of common sole model fishery-dependent data based on WAIC and LCPO scores. Time scores refer only to the estimation process of the model. The best model is highlighted in bold.

Parameter	estimate	cilow	ciupp	log.est
RUN 1				
<i>Bmsyd</i>	266.27011	75.49005	939.19361	5.584511
<i>Fmsyd</i>	15.77595	14.83957	16.77142	2.758487
<i>MSYd</i>	4200.66483	1246.62167	14154.72351	8.342998
<i>K</i>	4200.6648274	1246.6216654	1.415472e+04	8.3429981
<i>m</i>	532.5402196	150.9800969	1.878387e+03	6.2776584
RUN 2				
<i>Bmsyd</i>	3.324751e+05	512.828416	2.155490e+08	12.714320
<i>Fmsyd</i>	5.654210e-02	0.011523	2.774462e-01	-2.872769
<i>MSYd</i>	1.879885e+04	21.075496	1.676813e+07	9.841551
<i>m</i>	1.879885e+04	21.0754961	1.676813e+07	9.841551
<i>K</i>	6.649501e+05	1025.6568328	4.310981e+08	13.407467
RUN 3				
<i>Bmsyd</i>	1945.35	442.82	8546.08	7.57
<i>Fmsyd</i>	0.3525605	0.08096485	1.53522	-1.042533
<i>MSYd</i>	685.6973461	345.63207027	1360.35076	6.530436
<i>m</i>	7.073595e+02	359.48682933	1.391866e+03	6.5615390
<i>K</i>	3.964599e+03	904.04950017	1.738627e+04	8.2851601

Table 4: Parameter estimates (deterministic) and associated confidence intervals for MSY parameter m , carrying capacity k , biomass at MSY $Bmsyd$, fishing at MSY $Fmsyd$ and $MSYd$.

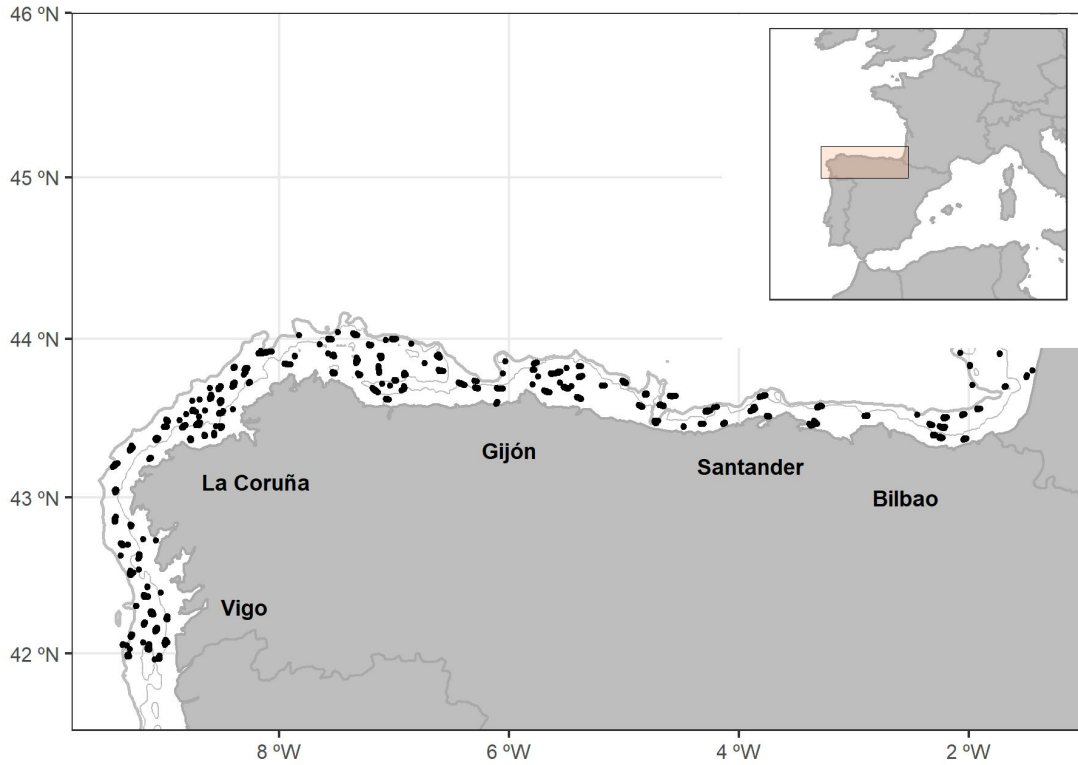


Figure 1: Map of the study area showing the distribution of the annual sampling locations of fishery-independent hauls.

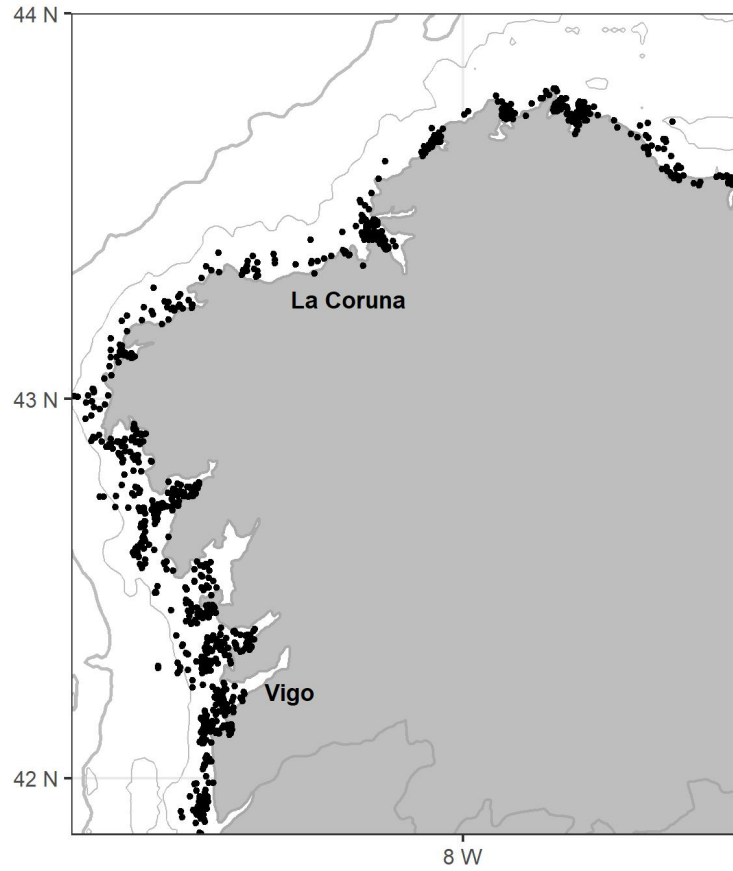


Figure 2: Map of the study area showing the distribution of the fishery-dependent sampling locations.

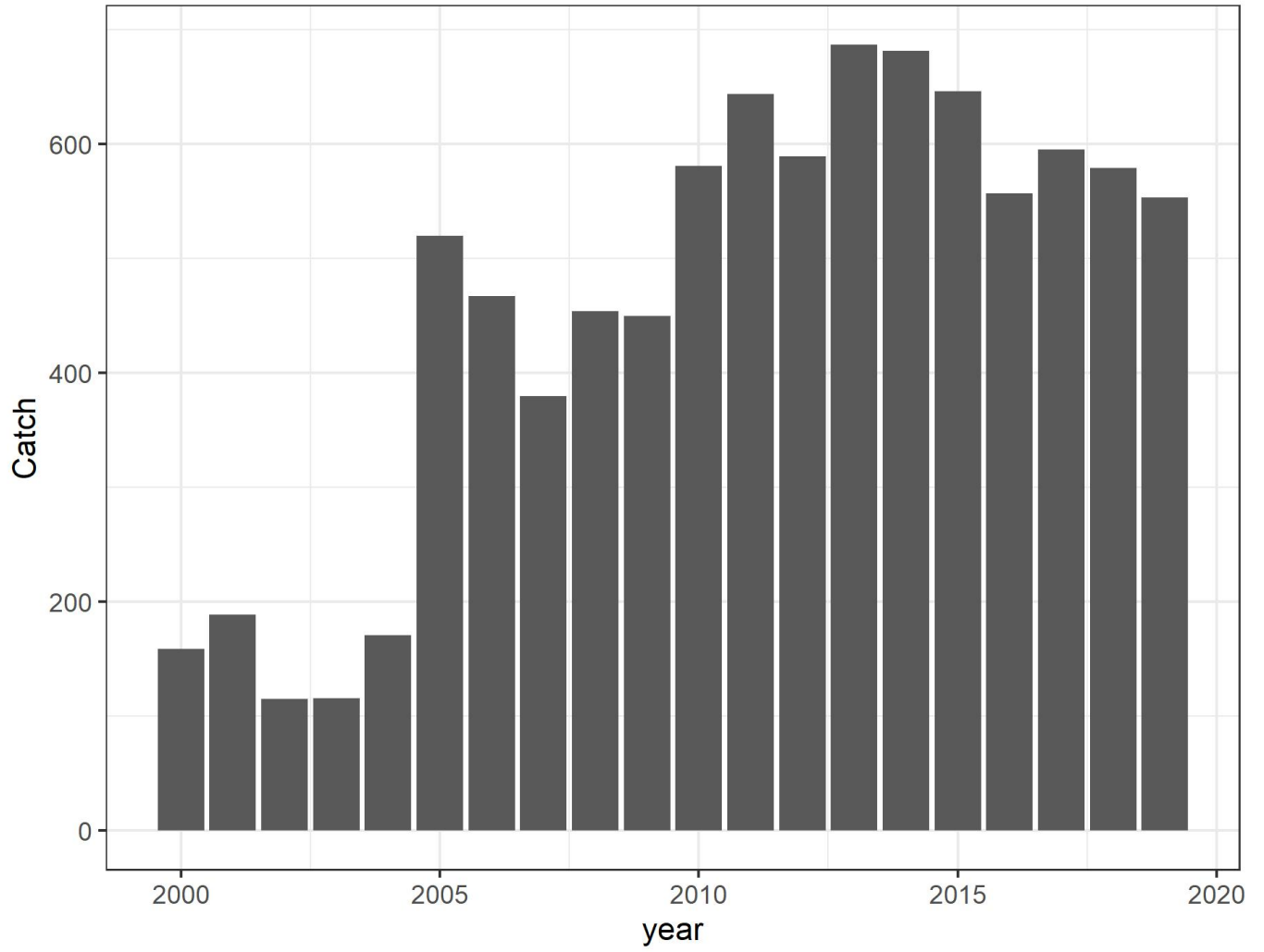


Figure 3: Common sole catch in ICES divisions 8.c and 9.a.

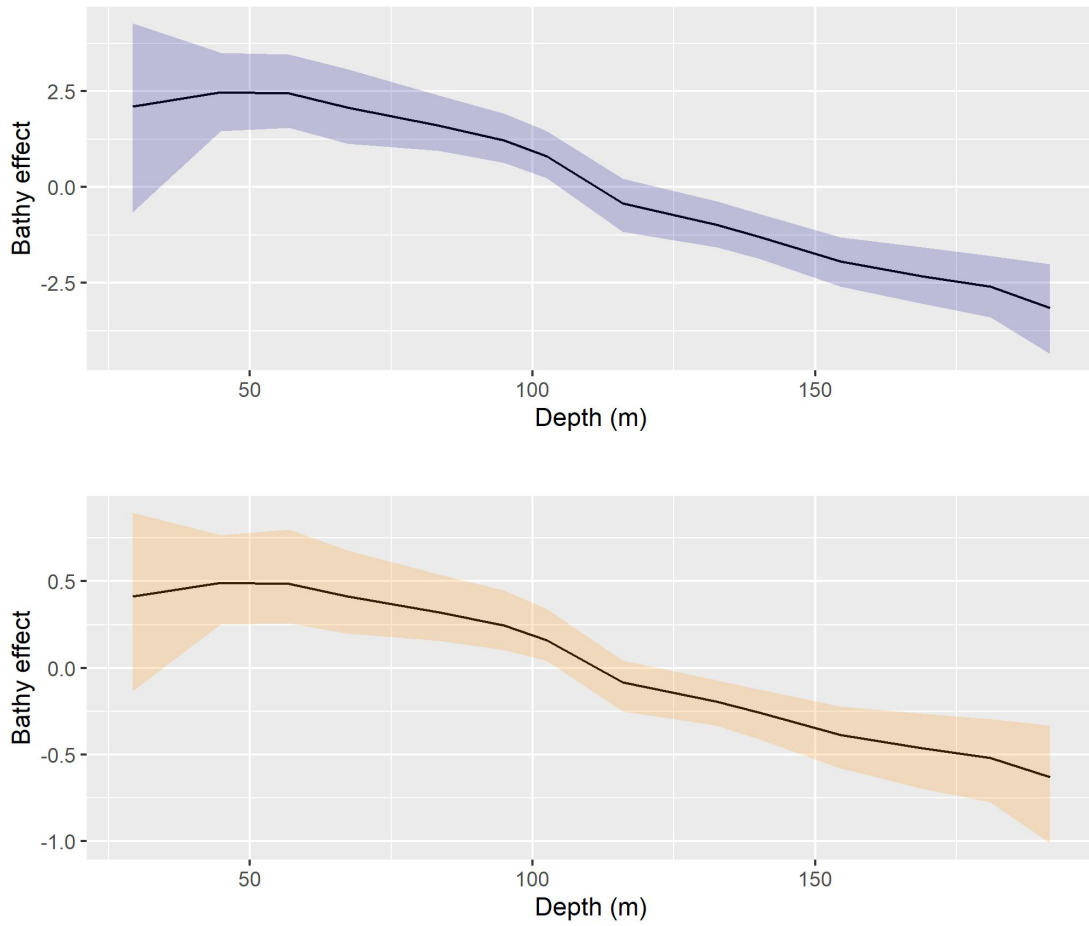


Figure 4: Smooth functions of the predicted occurrence (top) and abundance (bottom) for the bathymetry effect using fishery-independent data-set. The solid line is the smooth function estimate, and shaded regions represent the approximate 95% credibility interval.

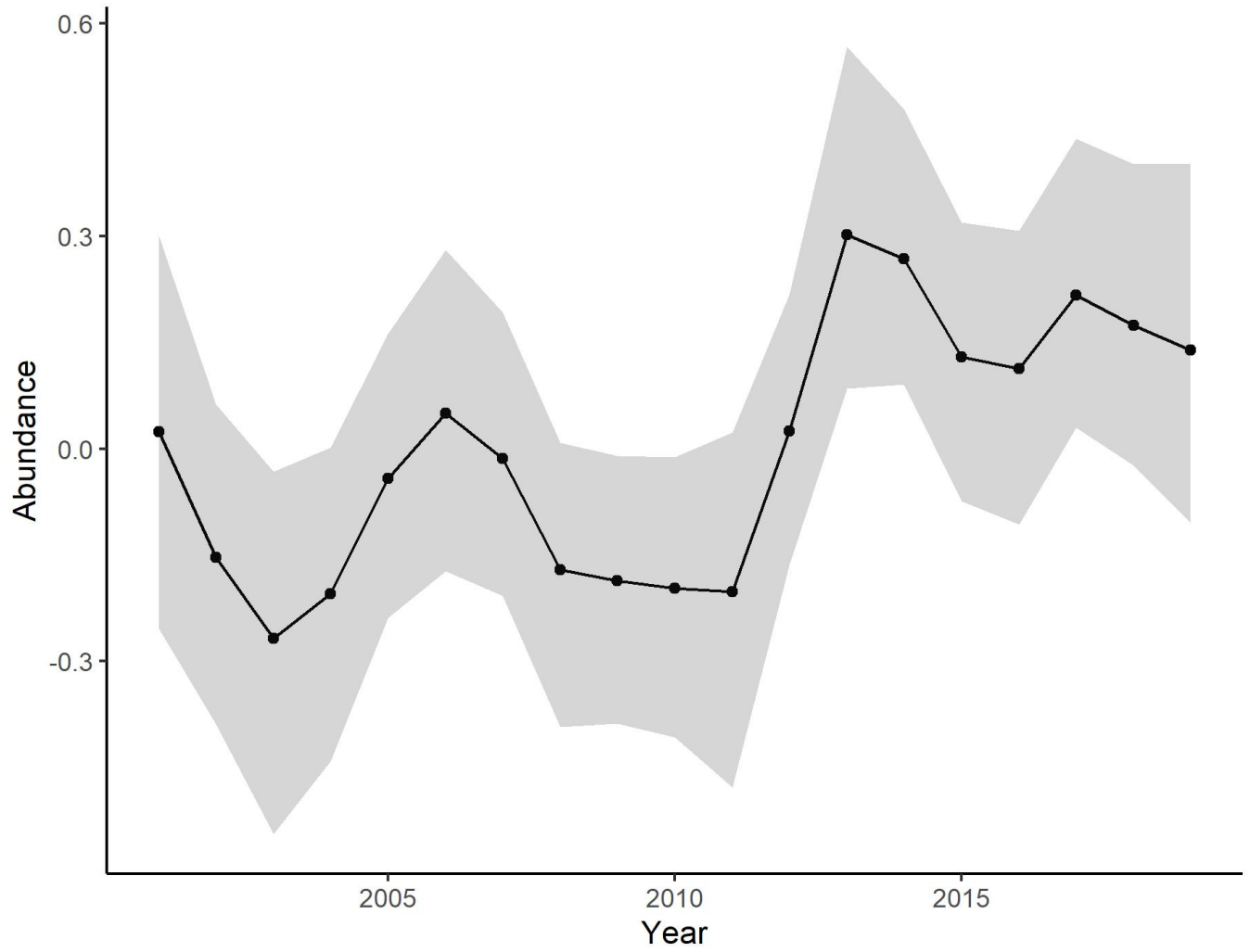


Figure 5: Marginal temporal effects in the linear predictor scale (logarithmic link) of common sole for fishery-independent data. Shaded regions represent the approximate 95% credibility interval.

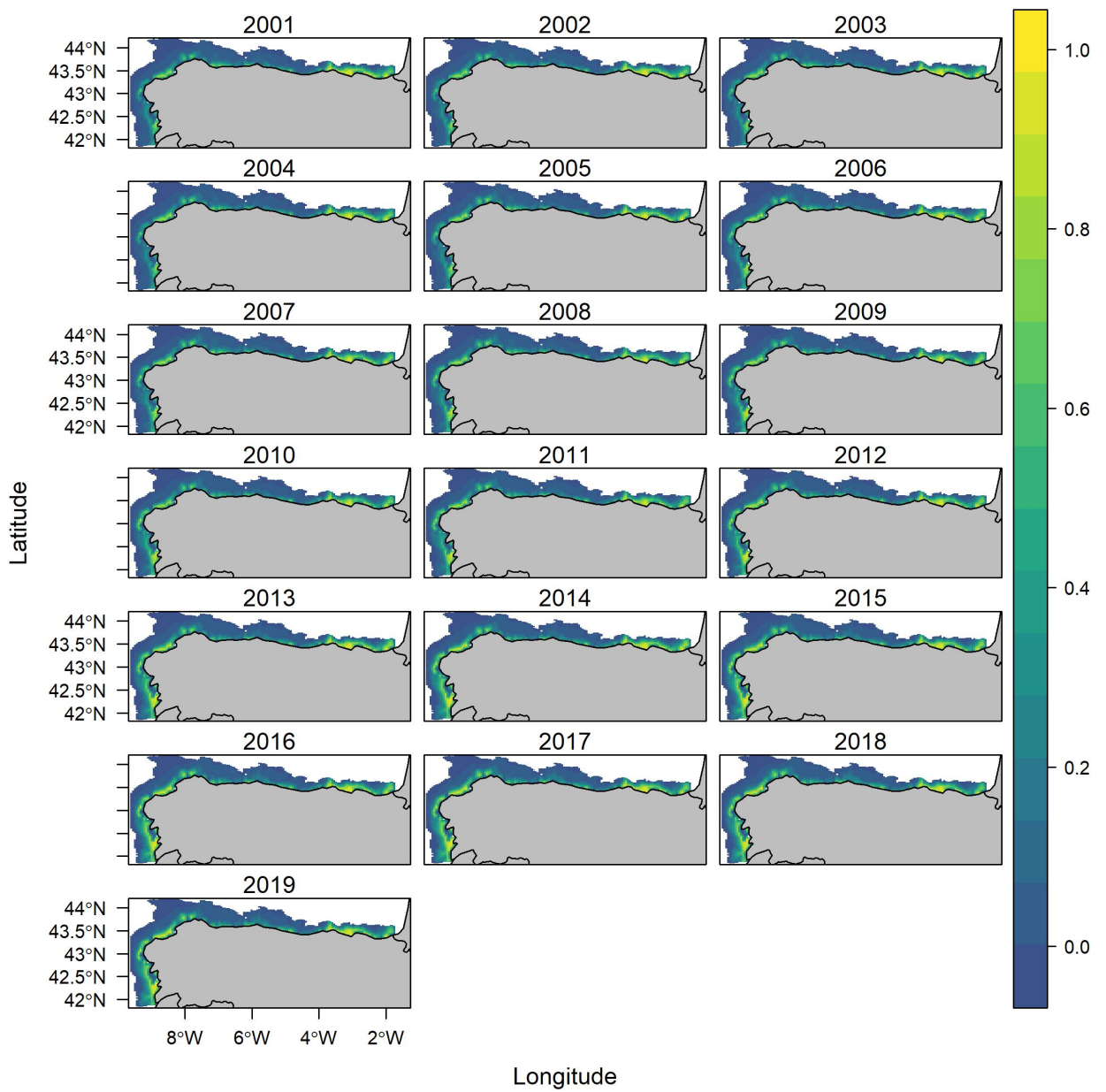


Figure 6: Prediction maps (2001-2019) of the common sole occurrence estimated by the hurdle Bayesian spatio-temporal model for fishery-independent data.

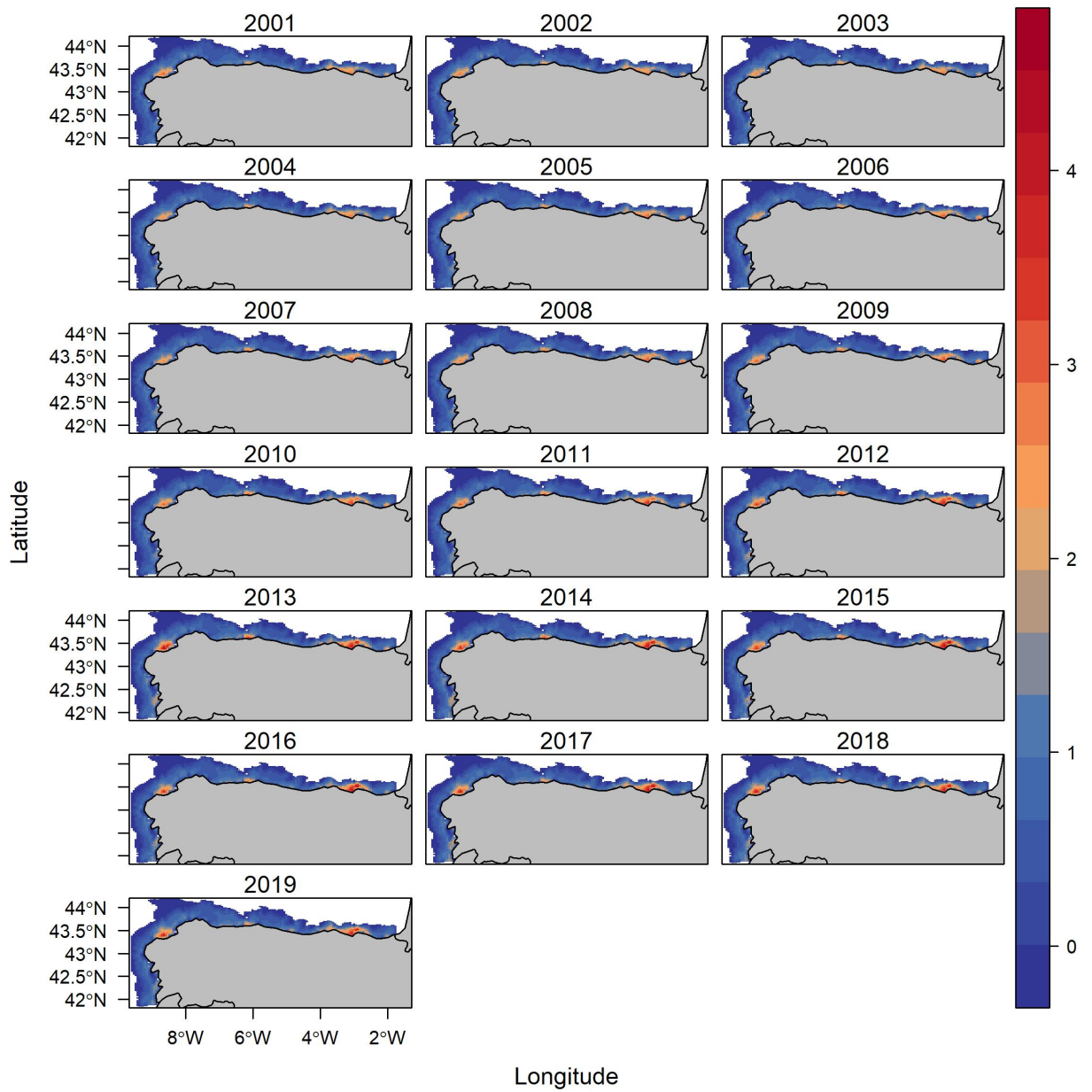


Figure 7: Prediction maps (2001-2019) of the common sole abundance estimated by the hurdle Bayesian spatio-temporal model for fishery-independent data.

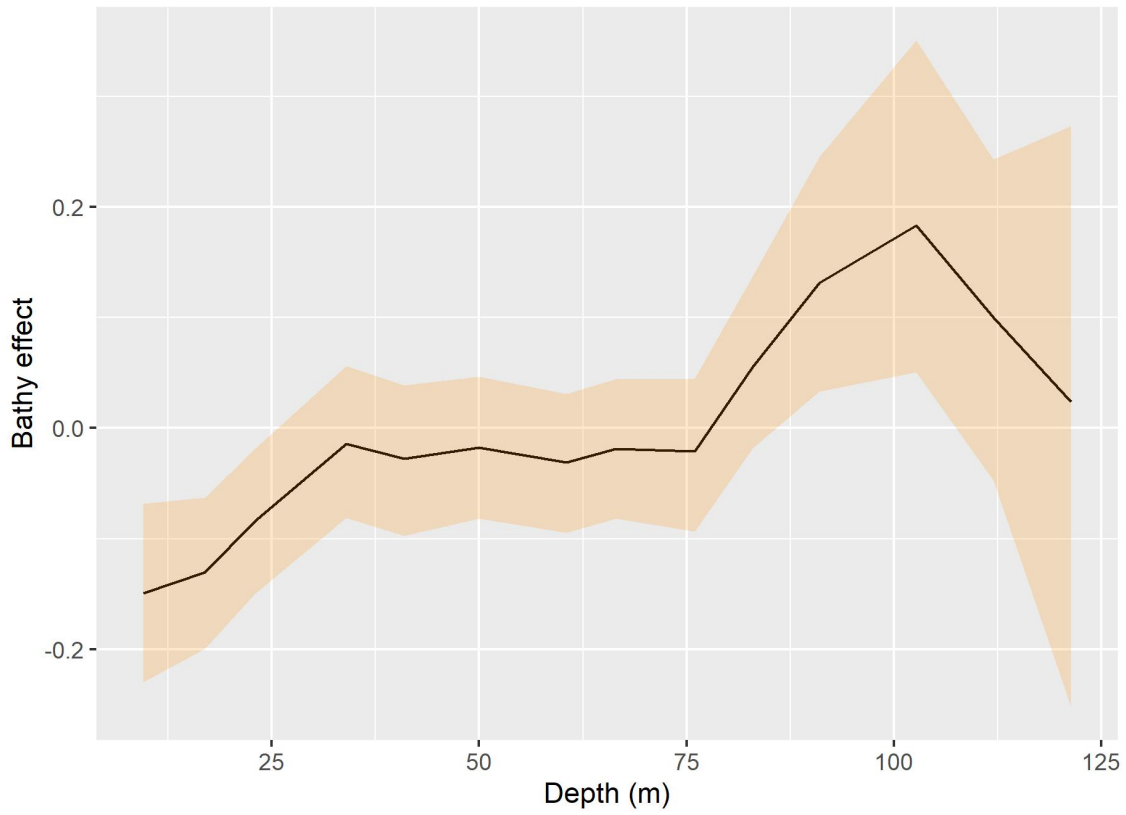


Figure 8: Smooth functions of the predicted abundance for the bathymetry effect using fishery-dependent data-set. The solid line is the smooth function estimate, and shaded regions represent the approximate 95% credibility interval.

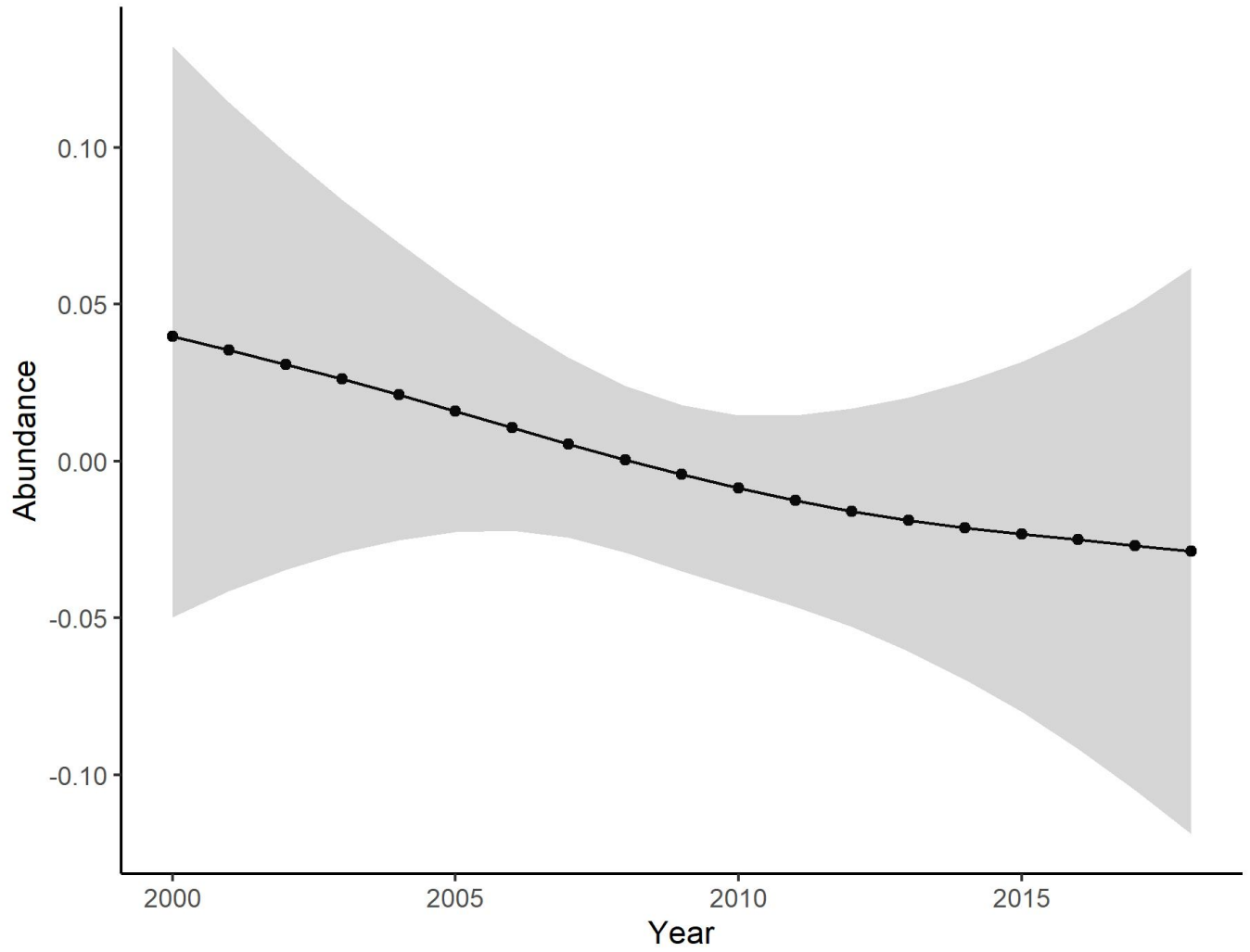


Figure 9: Marginal temporal effects in the linear predictor scale (logarithmic link) of common sole for fishery-dependent data. Shaded regions represent the approximate 95% credibility interval.

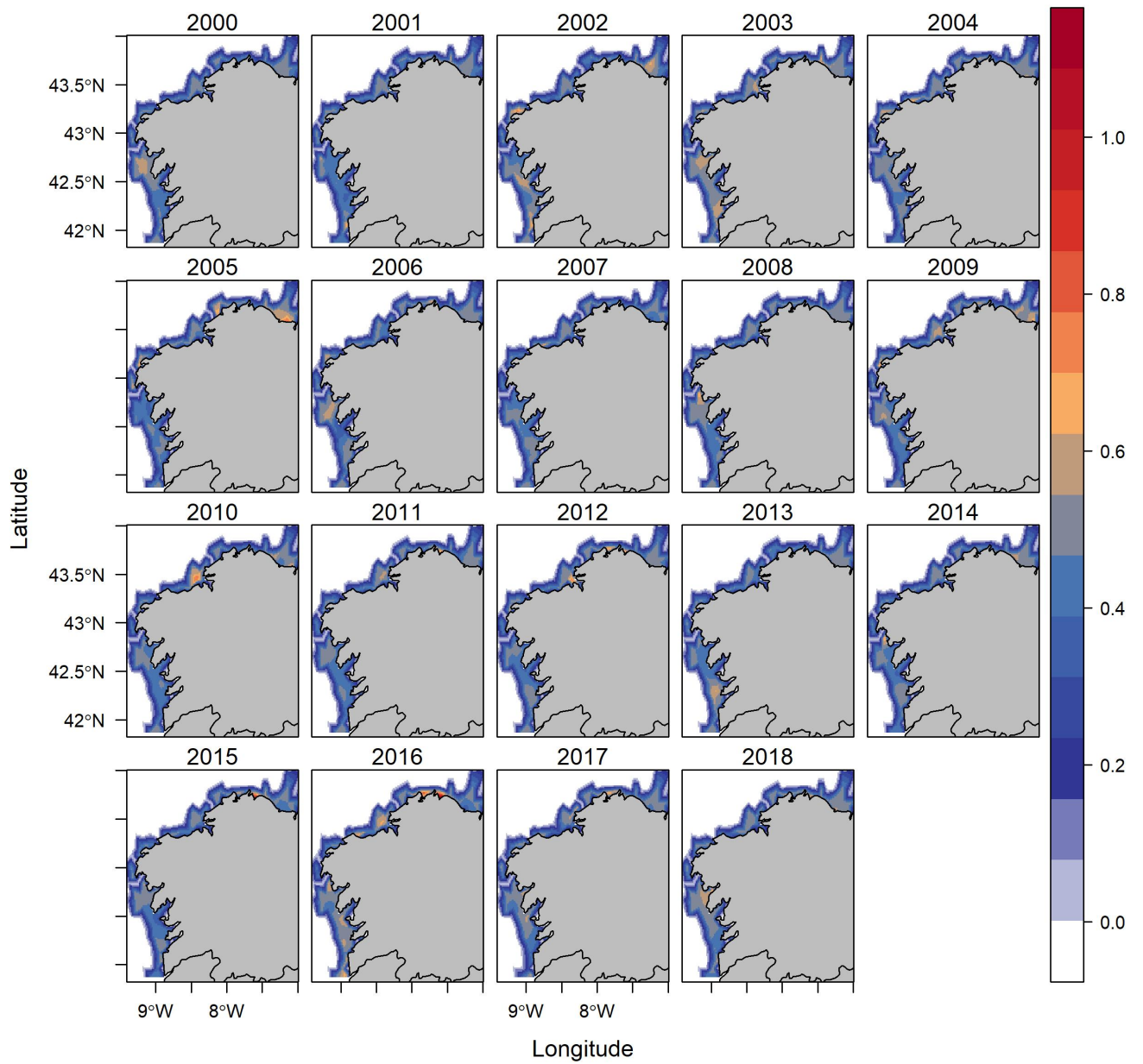


Figure 10: Prediction maps (2000-2018) of the common sole abundance estimated by the Bayesian spatio-temporal model for fishery-dependent data.

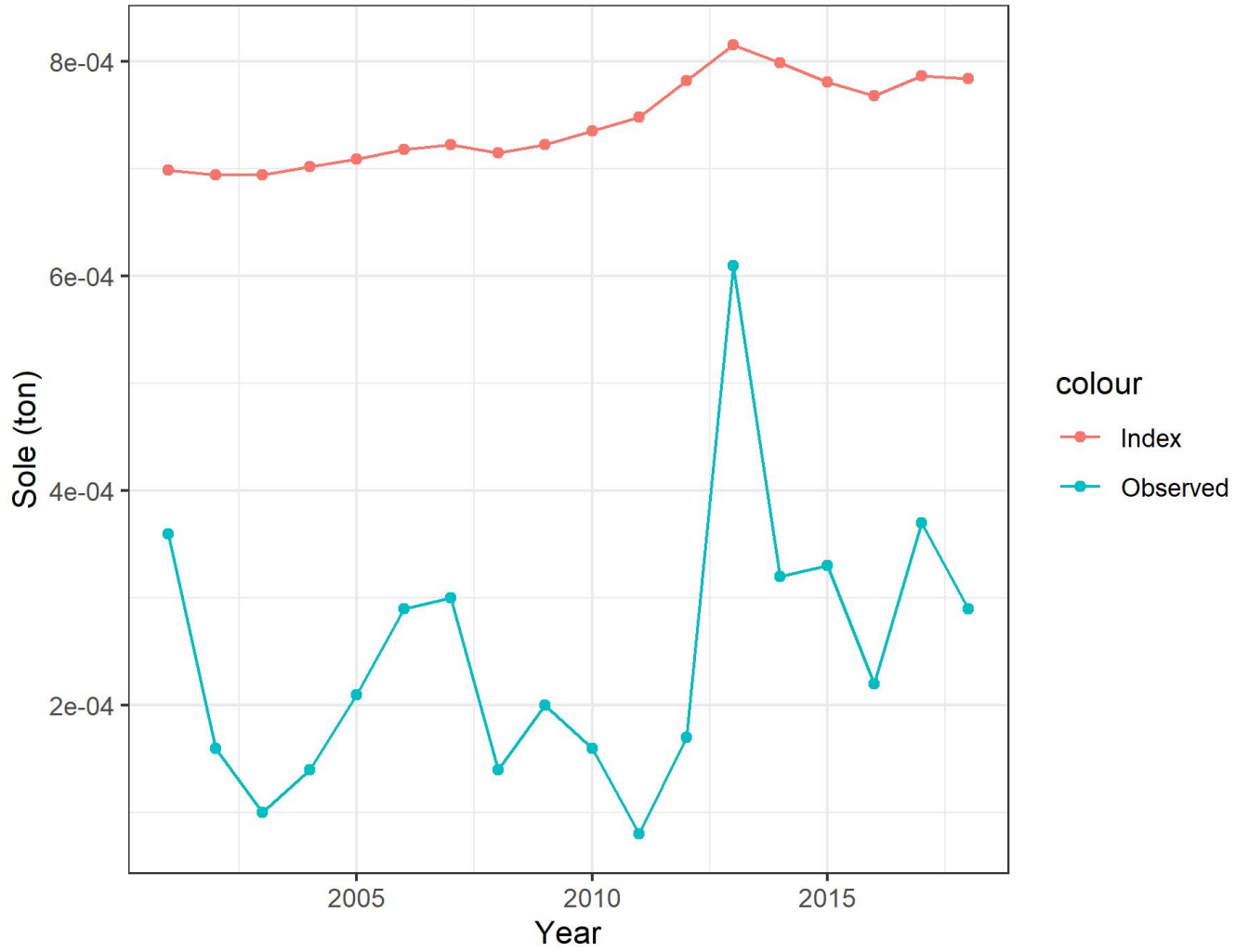


Figure 11: Spatio-temporal abundance index obtained for fishery-independent data (2001-2019) versus the survey abundance index standardized for the three bathymetric strata (i.e. 70–120 m, 121–200 m and 201–500 m).

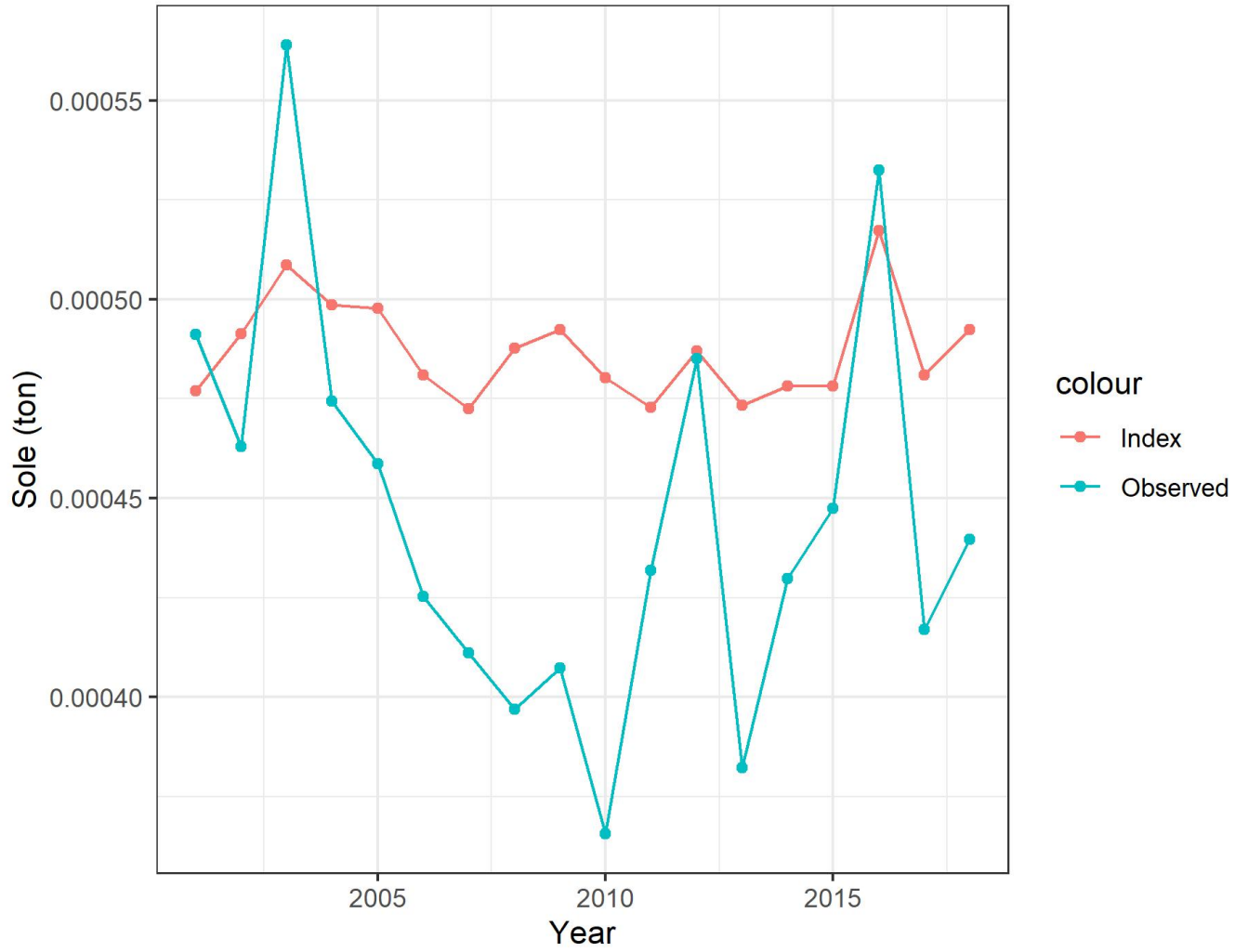


Figure 12: Spatio-temporal abundance index obtained for fishery-dependent data (2000-2018) versus observed fishery-dependent data.

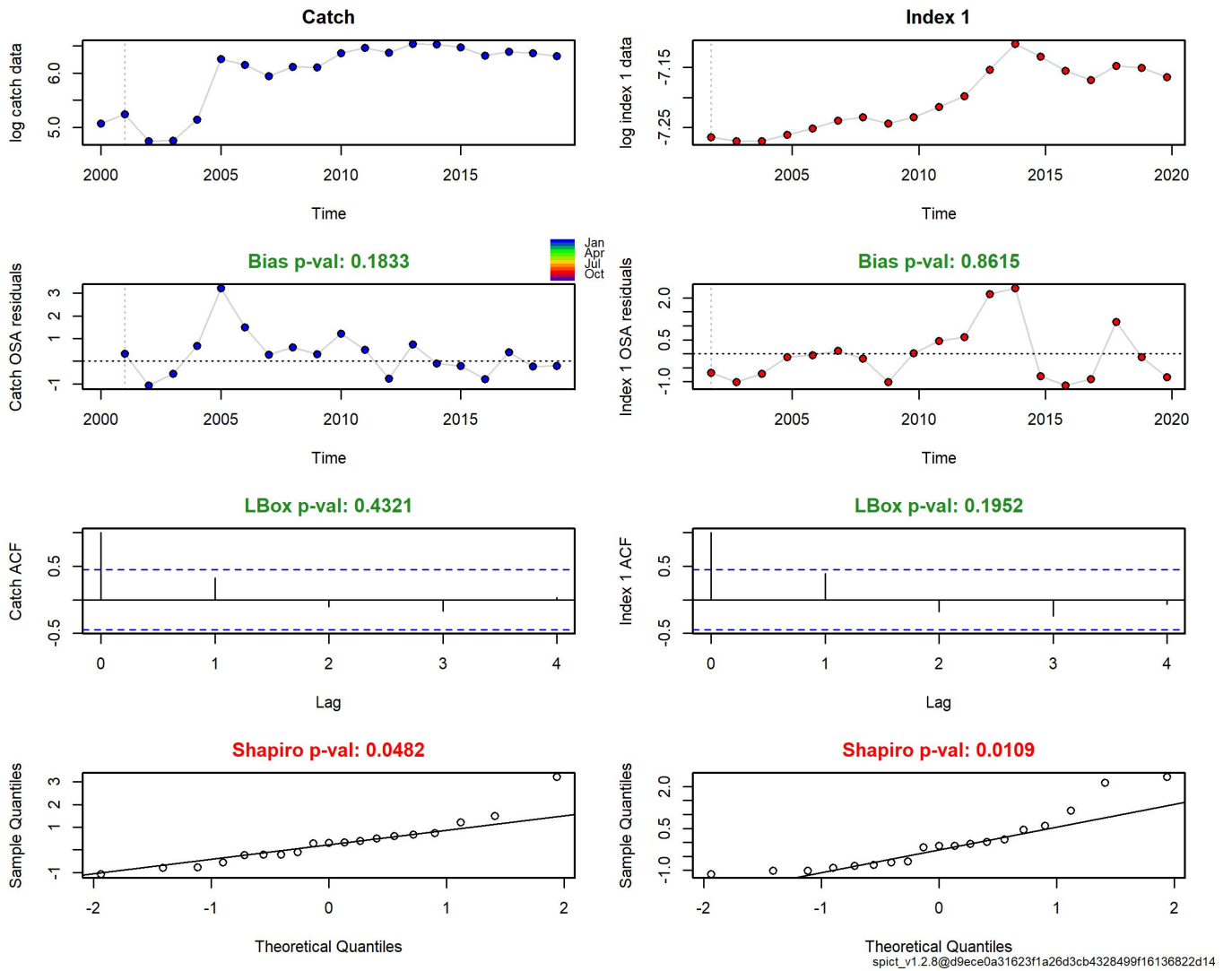


Figure 13: Standard OSA residuals for the run 1 surplus production model obtained using catch data and the spatio-temporal index of fishery-independent data.

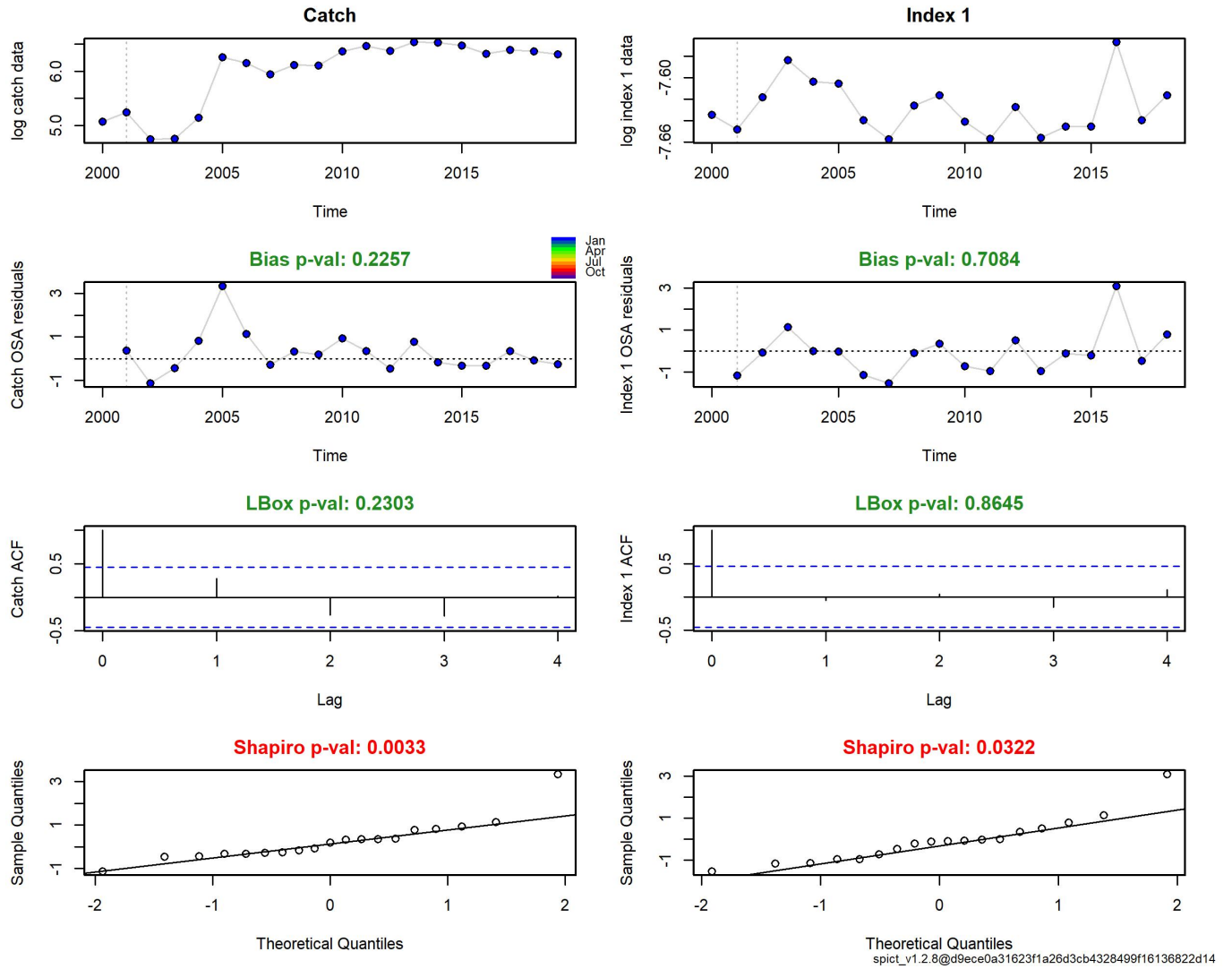


Figure 14: Standard OSA residuals for the run 2 surplus production model obtained using catch data and the spatio-temporal index of fishery-dependent data.

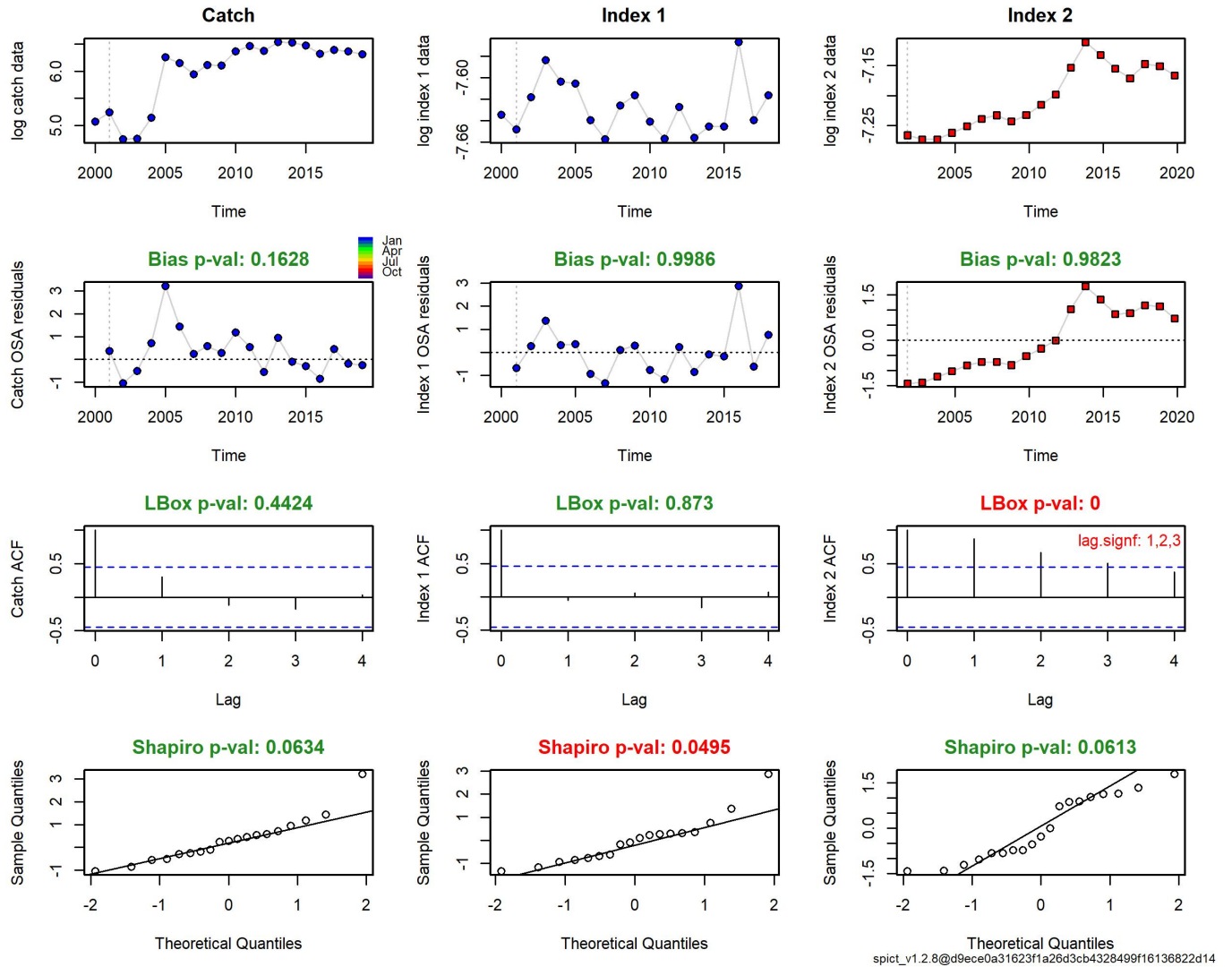


Figure 15: Standard OSA residuals for the run 2 surplus production model obtained using catch data and both spatio-temporal indices.